Trends in Applied Sciences Research

ISSN 1819-3579

Academic
Journals Inc.

www.academicjournals.com

Trends in Applied Sciences Research 8 (1): 14-25, 2013
ISSN 1819-3579 / DOI: 10.3923/tasr.2013.14.25
© 2013 Academic Journals Inc.

Effect of Shape Factor and Rubber Stiffness of Fiber-reinforced Elastomeric Bearings on the Vertical Stiffness of Isolators

Hossein Shakeri Soleimanloo and Mohammad Ali Barkhordari
School of Civil Engineering, Iran University of Science and Technology, Tehran, Iran

Corresponding Author: Hossein Shakeri Soleimanloo, School of Civil Engineering, Iran University of Science and Technology, Tehran, Iran

ABSTRACT

Shape factor of an elastomeric layer, main factor in designing isolators, is a measure of the local slenderness of the elastomeric bearing. In specific type of isolators named "steel like fiber-reinforced elastomeric isolators", special fibers such as fiber glass or carbon have been replaced steel plates, making them lighter than steel-reinforced elastomeric isolators and easier to produce. In this study, dynamic and mechanical behaviors of seven specimens of these isolators were modeled using finite element software (ABAQUS). Consequently, the effects of both shape factor and rubber stiffness of isolators on their vertical compression behavior were examined. The overall behavior of isolators found to be positively depended on the coefficient of shape factor and rubber stiffness, such that it increased by increasing both of them. To verify modeled outcomes, pre-existing laboratorial specimens were distinctly modeled by ABAQUS, followed by finite elements vertical tests. Comparison of finite elements vertical tests and pre-existing actual vertical tests showed that finite element software can precisely predict dynamic and mechanical behavior of fiber-reinforced elastomeric isolators.

Key words: Fiber-reinforced elastomeric isolator, vertical stiffness, vertical tes, shape factor, finite element modeling

INTRODUCTION

Seismic base isolation is a valuable earthquake-resistant technique for structures such as buildings and bridges. Seismic isolators with low horizontal, but high vertical and bending stiffness, increase the fundamental horizontal period of structure to a value beyond the dominant oscillation periods of earthquakes and attenuate transmitted earthquake energy to the structure considerably (Naeim and Kelly, 1999). Two types of common systems for seismic isolation for structures include; i.e., steel-reinforced multilayer elastomeric isolators and sliding bearings. In addition, other systems those are combination of these two types of bearings have been proposed (Naeim and Kelly, 1999).

A suitable laminated bearing with fabric layers for base isolation is characterized with high vertical stiffness and sufficient flexibility. Steel shells of isolators are heavy, expensive and rigid both in tension and bending and also involve complicated preparation methods (Kelly, 1999). Instead, all types of fiber-reinforced elastomeric isolators, made up of hard and strong cords of polymer Kevlar, fiber glass and carbon fibers, are much lighter than steel-reinforced isolators, have more tensional flexibility, have efficient adherence with rubber base and also completely lack bending stiffness (Kelly, 1999; Moon *et al*., 2002).

Kelly (1999) observed similar range of tilting and vertical stiffness for fiber-reinforced and steel-reinforced isolators with the same diameter and thickness of rubber. The proportion of shear stiffness and equivalent viscous damping of the, fiber-reinforced specimens to the steel-reinforced isolators also found to be 80 and 180%, respectively.

Comparison of fiber reinforced and steel reinforced isolator suggests a higher performance for carbon fiber reinforced isolator. Moon *et al.* (2002) reported that vertical stiffness, shear stiffness and equivalent viscous damping of the carbon fiber reinforced isolator were 299, 94 and 256% of corresponding parameters of the steel reinforced isolator, respectively.

Tsai (2004) proposed a closed form method to calculate the vertical stiffness of fiber-reinforced elastomeric bearings. The effects of bulk modulus, compressibility of base rubbers and boundary condition at the end of isolators were considered by the author in the elastomeric layer on the compression stiffness and performance of fiber-reinforced elastomeric bearings. The behavior of rubber layers and reinforcement layers found to be as linear elastic. This findings were consistent to the findings of another study by Tsai and Kelly (2005), in which they found a similar linear elastic behavior for the rubber layers and steel-reinforcement layers. They proposed a beam theory based on haringx theory (Haringx, 1948), to analyze mechanical characteristics, especially effective compression stiffness and the buckling load of the steel-reinforced elastomeric isolators. This method is also applicable to fiber-reinforced elastomeric isolators. The elastomeric layers also found to be incompressible.

Shape factor of isolator is an important factor to acquire suitable vertical stiffness and hence, to design resistant isolators. Since, the effect of shape factor on dynamic and mechanical behaviors of isolators and the optimum range of shape factors has not yet been studied thoroughly. This study sought to address this gap by evaluating the effect of shape factors on vertical stiffness of fiber-reinforced isolators and determining the suitable range of shape factors.

MATERIALS AND METHODS

In this study, different specimens of fiber-reinforced elastomeric isolators were modeled by ABAQUS software. Their mechanical characteristics were also examined using finite element analysis and vertical tests.

Vertical stiffness, shape factor and effective compression modulus: Three main mechanical characteristics of isolators are vertical, horizontal and bending stiffness. Vertical stiffness of an isolator was determined by designers using a static linear analysis under certain amount of load (Naeim and Kelly, 1999).

$$K_v = \frac{E_c A}{T_r} \quad (1)$$

Where:
K_v = Vertical stiffness of isolator under certain amount of load; E_c: effective compression modulus
A = Top surface; T_r: total thickness of isolator

The shape factor S of a rubber confined pad is the ratio between the loaded area and the lateral surface free to bulge. As shown in Fig.1, for a circular elastomeric bearing, the shape factor S was calculated by the following formula (Imbimbo and De Luca, 1998).

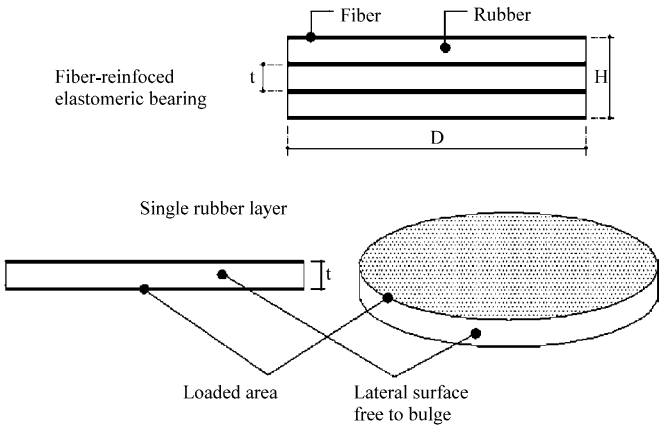

Fig.1: Shape factor of a confined rubber pad

$$S = \frac{\text{Loaded area}}{\text{Loaded area free to bulge}} = \frac{p \times D^2}{4} \times \frac{1}{pDt} = \frac{D}{4t} \tag{2}$$

where, D is the diameter of bearing and t is the thickness of single rubber layer.

Figure 1 shape factor of a confined rubber pad.

For a square shaped isolator (Imbimbo and De Luca, 1998):

$$S = \frac{\text{Loaded area}}{\text{Loaded area free to bulge}} = \frac{a \times a}{4 \times a \times t} = \frac{a}{4t} \tag{3}$$

Shape factor is measure of slenderness in a single rubber layer of the elastomeric bearing. This parameter highly affects the general slenderness of isolator, defined by the ratio of total bearing's height to the diameter of bearing (Imbimbo and De Luca, 1998).

Having a low shape factor of greater than 5 and less than 20, isolators exhibit a good isolation in both horizontal and vertical directions, whereas bearings with shape factor of greater than 20, show a good isolation only in the horizontal direction. This is obvious that low shape factors require much thicker layer of rubber to make them much more flexible. As a result, isolators adopted to seismic isolations generally have shape factor between 5 and 30 to provide a high vertical stiffness but low shear stiffness (Naeim and Kelly, 1999).

Reinforcing fibres produce a constraint on the free lateral expansion of the rubber. Having assumed the total incompressibility condition for a circular bearing, an equivalent compression modulus E_c was calculated for a given shape factor and rubber stiffness (Lindley, 1970):

$$E_c = E_0 (1+2kS) \tag{4}$$

With k being an empirical factor dependent on the rubber hardness.

Modelling techniques: The commercial Finite Element (FE) code ABAQUS was utilized to simulate main parameters influencing fiber-reinforced elastomeric bearings. Each simulated bearing, specified by a shape factor, was made of a rubber body with embedded carbon fiber layers. Simulated bearings varied in number of layers and rubber properties, particularly stiffness of

rubber. However, all models were identical in dimensions to be comparable with each other. Modeling steps included rubber and fiber material modeling, meshing the model and applying force.

At least seven specimens with different shape factors, but identical dimensions, including nine different types of rubber stiffness for each specimen, were modeled and tested. Table 1 shows main properties of modeled specimens.

Rubber: The hyper elastic Neo Hooke formulation (Simo and Pister, 1984) was adopted to model the incompressibility of rubber. This method, involved using two parameters of rubber: the bulk modulus K and the shear modulus G. Table 2 shows these parameters and rubber stiffness values adopted in this study.

Behavioral potential energy function of Neo-Hooke was calculated as:

$$U = C_{10}(\bar{I}_1 - 3) + \frac{1}{D_1}(J^{el} - 1)^2 \quad (5)$$

Where: U is the potential energy per unit volume, C_1, C_{10} are parameters independent of temperature J^{el} is elastic volume ratio. $\hat{I}_1$ is a valuable deviant strain that defined as follow:

$$\bar{I}_1 = \bar{\lambda}_1^2 + \bar{\lambda}_2^2 + \bar{\lambda}_3^2 = J^{-\frac{1}{3}}.\lambda_i \quad (6)$$

Table 1: Characteristics of the isolator specimens

Models number	Horizontal dimensions	Height	No. of Rubber layer	No. of Fiber layer	Rubber Thickness	Fiber Thickness	Total height of rubber	Total height of fiber	Models Number (S)
No.1	150×150	50.7	8	9	6	0.3	48	2.7	6.25
No.2	150×150	51.3	10	11	4.8	0.3	48	3.3	7.8125
No.3	150×150	51.9	13	14	4	0.3	48	3.9	9.375
No.4	150×150	49.8	16	17	3	0.3	45	4.8	12.5
No.5	150×150	50.9	23	24	2	0.3	44	6.9	18.75
No.6	150×150	50.7	29	30	1.5	0.3	42	8.7	25
No.7	150×150	49.9	33	34	1.25	0.3	40	9.9	30

All dimensions are in millimeters

Table 2: Stiffness of rubber (elastomeric) material

Hardness	G (Shear modulus, N mm^{-2})	E_b (Bulk modulus, N mm^{-2})
35	0.38	2000
40	0.45	2000
45	0.53	2030
50	0.63	2060
55	0.75	2090
60	0.89	2120
65	1.04	2150
70	1.22	2180
75	1.42	2210

N: unit of force (Newton)

where, λ_i is main strain, J is the ratio of deformed elastic volume per primary volume of material and:

$$\mu_0 = 2C_{10}, k_0 = \frac{2}{D_1} \tag{7}$$

where, μ_0 is primary shear module and k_0 is the bulk module.

Fibre: In this study reinforcements in the rubber matrix were modeled in a 3D model by utilizing a smeared approach with structural solid elements. A smeared concept describes the fabric as a continuous sheet with an equivalent cross-sectional area (Mordini and Strauss, 2008). Carbon fiber layers with crossed fibers, parallel-oriented to the specimen sides, were described as continuous sheets with an average thickness of 0.3 mm. The layers were modeled as a linear elastic orthotropic material with elastic modulus E for main directions and zero in-plane and Poisson coefficients v.

The fibers (with thickness about 0.3 mm) were twisted to made strings and then fiber textile was waved. Strings were assumed to be perpendicular and were waved in different angles. This approach provided different dimensions with various characteristic. Accordingly, fiber layers showed a perpendicular tensile behavior.

To model the behavior of fibers, they were assumed as an orthotropic layer with the same thickness. Orthotropic materials have same behavior in both directions (related to the direction of fiber strings) and different behavior in thickness direction (Mordini and Strauss, 2008). The behavior of orthotropic layers was defined by 9 component of elastic stiffness in software.

The stress- strain formulation of fiber layers is:

$$\begin{Bmatrix} s_{11} \\ s_{22} \\ s_{33} \\ s_{12} \\ s_{13} \\ s_{23} \end{Bmatrix} = \begin{bmatrix} D_{1111} & D_{1122} & D_{1133} & 0 & 0 & 0 \\ & D_{2222} & D_{2233} & 0 & 0 & 0 \\ & & D_{3333} & 0 & 0 & 0 \\ & & & D_{1212} & 0 & 0 \\ & & & & D_{1313} & 0 \\ & & & & & D_{2323} \end{bmatrix} \times \begin{Bmatrix} e_{11} \\ e_{22} \\ e_{33} \\ e_{12} \\ e_{13} \\ e_{23} \end{Bmatrix} = \left[D^{et}\right] \times \begin{Bmatrix} e_{11} \\ e_{22} \\ e_{33} \\ e_{12} \\ e_{13} \\ e_{23} \end{Bmatrix} \tag{8}$$

Carbon fiber parameters were used for modeling as shown in Table 3. It consists of elastic modulus E, shear modulus G and Poisson coefficient **v** in three dimensions. The shear modulus or modulus of rigidity (G) describes the tendency to shear (the deformation of shape at constant volume) when a force is applied parallel to one face of the object while the opposite face is held fixed. It is defined as shear stress over shear strain.

The elastic modulus, or modulus of elasticity, is the mathematical description of a substance's tendency to be deformed elastically under a given force. The elastic modulus of an object is defined as the slope of its stress-strain curve in the elastic deformation region.

Table 3: Characteristics of the carbon fibers

-GPa (T-300 , PAN)carbon fiber									
v23	v13	v12	G23	G13	G12	E3	E2	E1	Parameter
0.25	0.25	0.3	4.22	4.22	18.2	10.26	243.6	243.6	amount

T-300, PAN: Type of carbon fiber, GPa: unit of pressure (Gigapascal), E: Elastic modulus in three directions, G: Shear modulus in three directions and v: Poisson's ratio in three directions

Poisson's ratio (**v**) is the ratio of transverse contraction strain to longitudinal extension strain in the direction of stretching force.

Since characters of orthotropic materials were calculated in a local system, a local-matrixes coordinate system was defined for each layer. The following strain-stress matrix was calculated and applied in software.

$$10^3\begin{Bmatrix} 294.27 & 113.8 & 4.62 & 0 & 0 & 0 \\ & 294.27 & 4.62 & 0 & 0 & 0 \\ & & 12.93 & 0 & 0 & 0 \\ & & & 18.2 & 0 & 0 \\ & & & & 4.22 & 0 \\ & & & & & 4.22 \end{Bmatrix} \quad (9)$$

Vertical tests: To investigate the bearing behavior, the static analyses were performed in two steps: First, a vertical loading was gradually applied to the rubber up to a stress of about 67 KN. In the second step, vertical tests were performed using dynamic tension and pressure test with 20 KN attitudes. During these steps, the vertical stiffness (K_v) was recorded as functions of the vertical displacements. A total number of 63 static analyses for 3D models were performed.

Elements and meshes: Since rubber is a nearly incompressible material, the finite element (FE) mesh was designed with elements allowing a hybrid formulation. The loading condition and shape conditions of specimens were symmetrical so, the specimens were considered as 3D domains. The 8-node 3D solid elements with hybrid formulation C3D8H were used to simulate the rubber layers. Three layers of solid elements were used to mesh the rubber between the fiber layers (Fig. 2). The carbon fiber layers were modeled with the 8-node hybrid structural elements C3D8R, sharing their

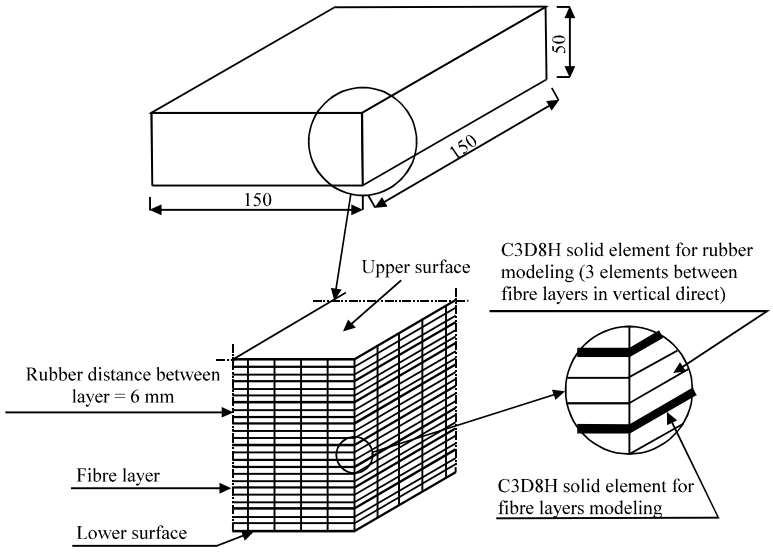

Fig. 2: Solid structural FE elements for specimens

nodes with the rubber elements. To provide a stable FE model, the bottom surface of models was constrained (both transformation and rotation in all directions) and loads were solely applied to the top surface of isolators. Considering selected solid structural elements, cube meshes were selected and meshing applied manually.

In vertical direction each rubber and each fiber were divided in to three and one meshes respectively. In horizontal direction they were also divided into 22 to 25 meshes to provide a suitable proportion between horizontal and vertical dimensions.

Verification of FE model: To ensure of running FE model in the accurate long, validity of model was tested via a distinct simulation. Specimens of carbon fiber reinforced elastomeric isolators, with different shape factors, were simulated by ABAQUS and compared with identical laboratorial specimens (Ashkezari *et al*., 2008). Design of specimens was based on uniform building code (UBC97). Rubber properties included 9 type of stiffness were selected based on American Association of State Highway and Transportation Officials code (AASHTO, 2001).

Effective compression modulus and vertical stiffness of isolator were calculated using the following relationship (Naeim and Kelly, 1999).

$$K_v = \frac{F_{max} - F_{max}}{\Delta_{max} - \Delta_{min}}, \quad E_c = \frac{K_v.T_r}{A_{horizontal}} \tag{10}$$

where, E_c is the effective compression modulus, k_v the vertical stiffness of isolator from test, A_h the cross-sectional area of a reinforcement layer and T_r is the total rubber thickness in isolator. F is vertical load related to liner part of graph and Δ is the amount of displacement for certain load.

RESULTS

Effective compression modulus of fiber-reinforced elastomeric isolators: Effective compression modulus of isolators found to be increased by increasing the shape factor of isolators and rubber stiffness. Results of tests are shown in Table 4. The table includes the results of 63 finite element vertical tests for a counterbalance of seven shape factors and nine different values of rubber stiffness. Compression modulus was derived by using equation presented in Eq.10.

Table 4: Effective compression modulus of all FE modeled specimens

Rubber characteristics		E_c (Effective compression modulus, Mpa)						
		NO1	NO2	NO3	NO4	NO5	NO6	NO7
Stiffness(shure A)	G_0	S = 6.25	S = 7.812	S = 9.375	S = 12.5	S = 18.75	S = 25	S = 30
35	0.38	93.74	123.05	139.46	204.56	329.38	434.26	576.91
40	0.45	103.72	133.95	156.1	217.13	341.48	470.84	626.02
45	0.53	113.36	145.7	170.07	237.5	369.78	511.19	673.81
50	0.63	124	159.7	186.38	259.31	399.17	559.12	731.31
55	0.75	135.65	175.5	205.06	285.3	444.6	604.44	790.08
60	0.89	148.5	190.06	224.51	311.64	484.43	661.08	859.13
65	1.04	163.37	211.77	244.1	340.13	526.53	713.56	921.78
70	1.22	177.83	231.42	267.46	369.21	569.85	768.45	983.21
75	1.42	188.87	247.8	291.1	401.23	614.04	832.5	1053.45

Shure A: Standard of rubbers classified by AASHTO, G_0: Initial shear modulus, S: Shape factor and MPa: unit of pressure (Megapascal)

According to this Table 4 an increase in shear modulus of rubber causes a significant growth in effective compression modulus of all models. For instance, in model no.1 (shape factor of 6.25) variation of shear modulus from 0.38 to 1.42 MPa results to an increase in effective compression elastic modulus from 93.74 to 188.87 MPa (101.48%). A slower growth is seen for isolators of higher shape factors, such that for isolator with shape factor S = 12.5, the effective compression modulus grows from 204.56 to 401.21 MPa (about 96.1%). This is even lower for isolator with shape factor S = 30, the effective compression modulus grows from 576.91 to 1053.45 MPa (about 82.6%). It can be derive that the effect of rubber stiffness for fiber-reinforced elastomeric isolators with high shape factor is less than isolators with low shape factor. Nevertheless, even for these isolators the effect of rubbers stiffness is considerable.

The higher shape factors also cause substantial increase in effective compression modulus of isolators. As an example, for isolators with similar rubber stiffness 35 shure A, the effective compression modulus increases from 93.74 to 576.91 MPa, along with growing up of shape factor from S = 6.25 to S = 30. Consistently for isolators with similar rubber stiffness (55 shure A) increases from 135.65 to 790.08 MPa by rising shape factor. In addition, the effective compression modulus grows up from 188.87 to 1053.45 MPa for isolators with higher rubber stiffness of 75 shure A.

Shape factor of fibre-reinforced elastomeric isolators: Vertical stiffness for all fiber-reinforced isolators found to be increased by increasing their shape factors (Table 5). Vertical stiffness was calculated by using equation presented in (Eq. 10). Rubbers characteristics are shown by their stiffness (shure A) and initial shear modulus of rubbers. The table includes the results of 63 finite element vertical tests for a counterbalance of seven shape factors and nine different values of rubber stiffness.

In all models an increase in initial shear modulus (G_0) of rubber (indicator of rubber stiffness), underlies a significant growth in vertical stiffness of isolator. For instance, in model no.1 with shape factor S = 6.25, the shear modulus grown up from 0.38 to 1.42 MPa (35 shure A to 75 shure A), resulted to an increase in vertical stiffness from 42 to 84 KN mm^{-1} (102%). This trend is slower for isolators with of higher shape factors, such that vertical stiffness increases from 92.42 KN mm^{-1} to 181.28 KN mm^{-1} (96.14%) for isolators with shape factor S =12.5 and from 260.13 to 303.82 KN mm^{-1} (82.6%) for isolator with shape factor S = 30.

Table 5: Vertical stiffness of all FE modeled specimens

Rubber characteristics		Vertical stiffness (KN mm^{-1})						
		NO1	NO2	NO3	NO4	NO5	NO6	NO7
Stiffness (shure A)	G_0	S = 6.25	S = 7.812	S = 9.375	S = 12.5	S = 18.75	S = 25	S = 30
35	0.38	41.6	53.97	60.46	92.42	145.6	192.72	260.13
40	0.45	46.03	58.75	67.67	98.102	150.95	208.95	282.27
45	0.53	50.4	63.9	73.73	107.3	163.46	226.86	303.82
50	0.63	55	70.04	80.8	117.16	176.45	248.13	329.75
55	0.75	60.2	76.98	88.9	128.9	195.53	268.24	356.25
60	0.89	65.92	83.5	97.33	140.8	214.14	293.38	387.38
65	1.04	72.5	92.8	105.82	153.67	232.75	316.67	415.63
70	1.22	78.52	101.5	115.95	166.81	251.9	341.03	443.33
75	1.42	83.82	108.7	126.2	181.28	271.43	369.45	475

Shure A: Standard of rubbers classified by AASHTO, G_0: Initial shear modulus, S: Shape factor and KN: unit of force (in Kilonewton)

Variations of vertical stiffness of isolators by increasing the shape factor and rubber stiffness found to be consistent to that shear modulus (G_0) of rubber. For all isolators with rubber stiffness 35 shure A, increasing the shape factor from 6.25 to 30, resulted in increasing the value of vertical stiffness from 41.6 to 260.13 KN mm^{-1}. Moreover, it can be seen from Table 5 that for isolators with rubber stiffness 55 shure A, growing the shape factor from 6.25 to 30, causes vertical stiffness to rise of from 60.2 to 356.25 KN mm^{-1}. Consistently, for isolators with rubber stiffness 75 shure A, vertical stiffness of isolators increases from 83.82 to 475 KN mm^{-1}. Overall, an increase in shape factor from 6.25 to 30 and rubber stiffness from 35 to 75 causes a considerable growth in vertical stiffness of isolators from 42 to 475 KN mm^{-1}.

Surprisingly there was a large variation in the vertical stiffness of bearings. The vertical stiffness of isolators found to be depended on the dimension, rubber stiffness and shape factor of isolators. Accordingly, without having knowledge about the construction process and the amount of vertical load produced by structure, it is difficult to explain the optimum ranges of rubber stiffness and shape factor. Therefore, one should make a balance between these parameters. However, shape factor between 5 and 30 can provide the suitable vertical stiffness.

Verification of FE model: The characteristics of laboratorial specimen modeled to verify the finite element method were:

Specimen dimension: 145×145

Number of rubber layer $n_r = 16$, number of fiber layer $n_f = 15$, rubber thickness $h_f = 2.59$ mm, fibber thickness $t_f = 0.25$ mm, total height of rubber $H_r = 41.5$ mm, shape factor S = 14.46.

To verify the finite element model these laboratorial specimens were modeled. After completing finite element, analyses were carried out to compare the FE method and experimental results. The vertical force versus displacement curves for vertical loading, performed by ABAQUS in this study is shown in Fig. 3.

From the Fig. 3, it may be observed that parts of the curves related to cyclic unloading and loadings are almost linear. It is also shown that the second and third cycles are almost coincident in each test (Toopchi-Nezhad *et al.*, 2008). Vertical stiffness of isolator was considered as the slope of the linear part of these curves. For two different levels of vertical loading, as load increases the curve becomes linear. At the beginning of test due to nonlinear behavior of materials under low

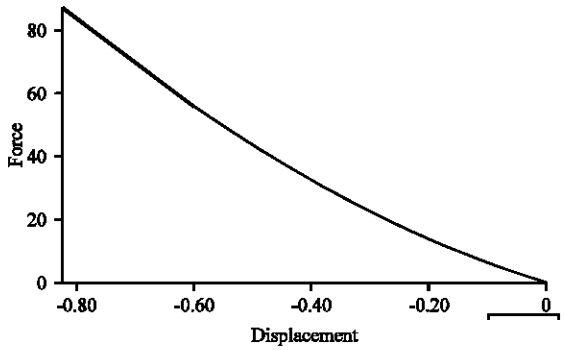

Fig. 3: The curve of load-vertical displacement (Finite element test with P = 67±20 KN)

Table 6: Vertical stiffness and efficient compression modulus of experimental and FE methods

	P = 67±20 KN		P = 135±35 KN	
Isolators specimens	K_v (KN mm^{-1})	E_c (MPa)	K_v (KN mm^{-1})	E_c (Mpa)
Experimental test	133.33	263.18	155.90	307.73
Finite element test	135.05	266.2	154.7	305.3

P: Pressure, KN: Unit of force (in Kilonewton), K_v: vertical stiffness, E_c: compression modulus, MPa: Unit of pressure (in Megapascal)

loads and low flexibility of fibers, the curve was nonlinear. In high level of loading, temporary nonlinear behavior of elastomeric isolator turned to linear. As a result, the whole behavior of isolator became linear.

Table 6 compares the results of experimental study derived by Ashkezari *et al.* (2008) and finite element tests in this study for two levels of load. Results suggest that experimental vertical stiffness are 133.33 KN mm^{-1} under vertical load P = 67±20 KN and 155.90 KN mm^{-1} under vertical load P = 135±35 KN, while vertical stiffness of isolators derived by FE method in this study are 135.05 KN mm^{-1} under vertical load P = 67±20 KN and 154.7 KN mm^{-1} under vertical load P = 135±35 KN. Compression modulus derived by experimental method are 263.18 and 307.73 MPa under vertical loads of P = 67±20 and P = 135±35 KN, respectively. The compression modulus calculated by FE method in this study are 266.2 MPa under vertical load P = 67±20 KN and 305.3 MPa under load P = 135±35 KN.

As it can be seen the vertical stiffness and compression modulus of elasticity from experimental and finite element methods are close together. The results highlight that finite element method has the potential for modeling and investigating mechanical characteristics of fiber-reinforced isolators.

DISCUSSION

In this study, some specimens of multilayer elastomeric seismic isolators, reinforced by layers of woven carbon fibers, were modeled by finite element software. Consequently, the effects of shape factor and rubber stiffness on vertical stiffness and effective compression modulus of these isolators were examined.

Vertical stiffness and effective compression modulus of the carbon-fiber-reinforced elastomeric isolators found to be positively influenced by shape factor. Such that, by increasing the shape factor from S = 6.25 to S = 30, both values of effective compression modulus and vertical stiffness of isolator increased from 60.2 to 356.25 (around 492%) for isolators with rubber stiffness 55 shure A. These findings are in good agreement with findings of a similar FE method study on fiber-reinforced bearings by Kelly and Calabrese (2012). They reported a similar variation of effective compression modulus from 97 to 522 (around 438%) for shape factors from 10-30.

In this study an increase of 71% in vertical stiffness of isolators with shape factor from 18.75 to 30, found to be a little different from findings of Ashkezari *et al.* (2008), who found an increase of 43% in vertical stiffness for the shape factor from 14.5 to 39.8. The difference could be from different factors, such as the smaller dimension of isolators adopted in their study, different amount of vertical load applied to the isolators and different range of shape factors.

In this study effective compression modulus showed a different increment slope for two ranges of shape factors. The effective compression modulus for isolators with 75 shure A increased about 251% by increasing the shape factor from 6.25 to 18.75, while it arouse more slowly about 71% when shape factor ranged from 18.75 to 30 (Table 4). Tsai and Kelly (2001), reported a similar

trend, but different values of compression modulus for circular bearings. According to their findings, for isolator with smaller shape factors from 5 to 20 the effective compression modulus varied from 98 to 336 (242%), while it had a slower variation from 336 to 560 (67%) for shape factor from 20 to 100. These differences in values of effective compression modulus could be attributed to the shape of isolators and the methods of solution.

Vertical stiffness also found to have different increase rates for different ranges of shape factors. Vertical stiffness of isolators with the same standard rubber stiffness of 35 shure A, increased around 250% by variation of shape factor from 6.25 to 18.75, but it increased more slowly around 78% for shape factor from 18.75 to 30 (Table 5). Studies by Pinarbashi and Yalchin (2008) and Kelly and Takhirov (2001) theoretically confirms this fact that the behavior of a low-shape factor layer may be considerably different from that of a high-shape factor layer.

Investigation of the effect of rubbers stiffness of isolators indicates that raising the stiffness of rubbers increases the value of vertical stiffness for fiber reinforced isolators. By increasing the stiffness of rubbers from 35 to 75 shure A, the value of vertical stiffness has increased out 96 percent. Moreover, for models with 35 shure A, by increasing the shape factor from 6.25 to 30, the effective compression modulus increases by about 515%. These findings are hardly comparable to other studies due to lack of sufficient information. However, the relations found and proposed by both Kelly (1999) and Tsai (2004) confirm these trends.

There was a good agreement between experimental tests and FE Modeling Results. However, validity of FE Modeling method needs to be tested using more actual specimens.

Considering that fiber-reinforced elastomeric bearings have significant vertical stiffness, lower weight and simple manufacturing procedure, these isolators have high potential for being a cost-effective method of base isolation. Nevertheless, optimum range of shape factor and vertical stiffness of these isolators steel remains to be determined. In this study damage condition, distribution of stress between layers, horizontal stiffness and the conditions of connection to the structures were not studied. These conditions need to be investigated in upcoming studies.

CONCLUSION

Shape factor and rubber stiffness of fiber-reinforced elastomeric are the main factors in manufacturing and designing isolators, such that they substantially influence vertical stiffness of isolators. Therefore, their applicability in designing earthquake resistant structures should be taken in especial consideration.

Comparison of experimental and FE modeling outcomes strengthens this idea that instead of handling experimental test to investigate characteristic of isolators, it is possible to use FE modeling methods for more study of isolators. Finite element method also provides a cost-effective procedure to probe influences of different rubber stiffness and shape factors on behavior of fiber-reinforced isolators.

REFERENCES

AASHTO, 2001. Guide Specifications for Seismiv Isolation Design. AASHTO, Washington, DC.

Ashkezari, G.D., A.A. Aghakouchak and M. Kokabi, 2008. Design, manufacturing and evaluation of the performance of steel like fiber reinforced elastomeric seismic isolators. J. Mater. Process. Technol., 197: 140-150.

Haringx, J.A., 1948. On highly compressive helical springs and rubber rods and their application for vibration-free mountings. Philips Res. Rep., 3: 401-449.

Imbimbo, M. and A. De Luca, 1998. F.E stress analysis of rubber bearings under axial loads. Comput. Struct., 68: 31-39.

Kelly, J.M., 1999. Analysis of fiber-reinforced elastomeric isolators. J. Seismol. Earthquake Engine., 2: 19-34.

Kelly, J.M. and S.M. Takhirov, 2001. Analytical and Experimental Study of Fiber-Reinforced Elastomeric Isolators. University of California, Berkeley.

Kelly, J.M. and A. Calabrese, 2012. Mechanics of fiber reinforced bearings. Pacific Earthquake Engineering Research Center. http://www.ntis.gov/search/product.aspx?ABBR=PB2013101798.

Lindley, P.B., 1970. Engineering design with natural rubber. Natural Rubber Technical Bulletin, 3rd Edn., Published by the Natural Rubber Producers Research Association.

Moon, B.Y., G.J. Kang, B.S. Kang and J.M. Kelly, 2002. Design and manufacturing of fiber reinforced elastomeric isolator for seismic isolation. J. Mater. Process. Technol., 130-131: 145-150.

Mordini, A. and A. Strauss, 2008. An innovative earthquake isolation system using fiber reinforced rubber bearings. Eng. Struct., 30: 2739-2751.

Naeim, F. and J.M. Kelly, 1999. Design of Seismic Isolated Structures. John Wiley and Sons, New York, Pages: 304.

Pinarbashi, S. and M. Yalchin, 2008. Elastic layers bonded to flexible reinforments. Int. J. Solids Struct., 45: 794-820.

Simo, J.C. and K.S. Pister, 1984. Remarks on rate constitutive equations for finite deformation problems: Computational implications. Comput. Meth. Applied Mech. Engine., 46: 201-215.

Toopchi-Nezhad, H., M.J. Tait and R.G. Drysdale, 2008. Testing and modeling of square carbon fiber-reinforced elastomeric seismic isolators. Struct. Control Health Monit., 15: 876-900.

Tsai, H.C. and J.M. Kelly, 2001. Stiffness analysis of fiber-reinforced elastomeric isolators. Pacific Earthquake Engineering Research Center, PEER report 2001/05. Berkeley CA, USA.

Tsai, H.C., 2004. Compression stiffness of infinite-strip bearings of laminated elastic material interleaving with flexible reinforcements. Int. J. Solids Struct., 41: 6647-6660.

Tsai, H.C. and J.M. Kelly, 2005. Buckling load of seismic isolators affected by flexibility of reinforcement. Int. J. Solids Struct., 42: 255-269.